0270-6474/83/0301-0133$02.00/0

The Journal of Neuroscience
Vol. 3, No. 1, pp. 133-144
January 1983

LOSS OF AXONS IN THE CAT OPTIC NERVE FOLLOWING FETAL UNILATERAL ENUCLEATION: AN ELECTRON MICROSCOPIC ANALYSIS[1]

ROBERT W. WILLIAMS,*,[2] MICHAEL J. BASTIANI,‡ AND LEO M. CHALUPA*

* *Department of Psychology and the Physiology Graduate Group, University of California, Davis, California 95616 and* ‡*Department of Biological Sciences, Stanford University, Stanford, California 94305*

Received April 7, 1982; Revised July 19, 1982; Accepted July 21, 1982

Abstract

Between the 48th day of gestation (E-48) and maturity, the number of axons in the cat optic nerve is reduced by approximately 50%. On the basis of an electron microscopic assay, the axon population of the E-48 nerve was estimated to be 328,000. In contrast, estimates from two normal adults were 159,000 and 158,000. *In utero* unilateral enucleation (at E-45 and E-46) attenuated the severity of this loss since the optic nerves of the experimental animals contained 200,000 and 198,000 fibers. These results indicate that prenatal binocular competition is involved in the elimination of ganglion cell axons during the normal development of the cat's visual system. The increased number of axons in the optic nerve of the prenatally enucleated animals could be due to reduced ganglion cell death or a failure to retract supernumerary axon collaterals. It is suggested that the former explanation is more consistent with what is currently known about the development of retinofugal projections.

Early in development, retinal projections to the dorsal lateral geniculate nucleus and the superior colliculus are diffuse (Rakic, 1976, 1977; Cavalcante and Rocha-Miranda, 1978; Frost et al., 1979; Land and Lund, 1979; Linden et al., 1981; Williams and Chalupa, 1982a), whereas the mature connections are characterized by distinct ocular dominance domains and an exquisite topography. The mechanisms which underlie this remarkable transformation are unknown. However, recent studies suggest that cell death may contribute to the development of the mammalian visual system and, in particular, to the refinement of patterns of connection (Cunningham et al., 1979, 1981; Jeffery and Perry, 1981; Sengelaub and Finlay, 1981, 1982; Stone et al., 1982). If ganglion cell death underlies the restructuring of retinal projections that we and others have recently demonstrated in the cat (Shatz and DiBerardino, 1980; Kliot and Shatz, 1981; Williams and Chalupa, 1980, 1981, 1982a), then the optic nerve of the fetus must contain a greater number of fibers than that of the adult. Furthermore, if this attrition is related to axon-target interactions, then prenatal unilateral enucleation should attenuate the severity of *in utero* retinal cell loss since the number of potential postsynaptic target sites available to axons of the spared eye could be doubled (cf. Rakic, 1979). The results of the present study are consistent with both of these ideas. We have found a significant attrition in the population of retinal ganglion cell axons during normal development. This loss is attenuated by the elimination of prenatal binocular competition.

Materials and Methods

Five cats were used in this study. Two were normal adults: a 10-month-old 2.5-kg female tabby and an 18-month-old 3.8-kg black and white male. The two experimental animals had one eye removed more than 2 weeks before their natural birth, one on embryonic day 45 (E-45), the other on day E-46, and were both born on the 63rd day of gestation. These unilateral enucleates were males with black and white coats. They were sacrificed 218 and 75 days after birth, at which time they weighed 2.7 and 0.8 kg, respectively. (These experimental animals are referred to as UNI-A and UNI-B.) The fifth animal was an E-48 fetus. The methods for obtaining timed pregnancies and the *in utero* surgical procedures have been described previously (Williams and Chalupa, 1982a).

[1] We wish to thank Dr. D. M. Hyde, Department of Anatomy, School of Veterinary Medicine, University of California, Davis, CA, for an appraisal of the sampling, counting, and analytic techniques used in this study. We also thank Fran Thomas of the Stanford University Department of Biological Sciences electron microscope facility for technical assistance. This research was supported by National Institutes of Health Traineeship GM 07416 to R. W. W., National Institutes of Health Postdoctoral Fellowship 1F32NS 06730-01 to M. J. B., and National Eye Institute Research Grant EYO-3991 to L. M. C.

[2] To whom correspondence should be addressed at Department of Psychology, University of California, Davis, CA 95616.

Tissue processing. The animals were perfused with physiological saline followed by a mixture of paraformaldehyde and glutaraldehyde in 0.1 M phosphate buffer (pH 7.3). For UNI-A a 1.0% paraformaldehyde/2.5% glutaraldehyde mixture was used, for UNI-B both fixatives were at a concentration of 2.5%, and in the normal animals as well as in the E-48 fetus, the perfusants were 4.0% paraformaldehyde/0.5% glutaraldehyde. The proportions of the fixatives were varied in an attempt to improve the preservation of axon sheaths. The most satisfactory fixation was obtained in UNI-A. However, even in this specimen the myelin sheaths, particularly those of the largest caliber axons, showed patches of delamination. Nevertheless, in all cases the fixation was uniform throughout the optic nerve and was of sufficiently high quality so that we could make an unequivocal distinction between axons and glial processes.

Within 1 hr of fixation the eye, optic nerve, and chiasm were exposed and immediately immersed in cold fixative. A portion of the optic nerve 1 to 2 mm in length was cut out, rinsed in phosphate buffer, and postfixed in a fresh 2% osmium tetraoxide solution. With the exception of UNI-A, all sections were taken from an intraorbital portion of the nerve close to the site of the optic canal (Fig. 1). This region of the nerve generally has a smaller cross-sectional area than portions closer to the eye or chiasm (our observations; Treff et al., 1972). The ultrathin section from UNI-A was cut as close as possible to the eye, within 500 μm of the lamina cribrosa. The tissue was stained in 2% uranyl acetate, dehydrated, and embedded in Epon-Araldite. The block was trimmed and angled in the chuck so that the cutting plane was parallel to a transverse section of the nerve. A 1-μm-thick section was cut before and after taking the ultrathin sections. Thick sections were stained using the Richardson et al. (1960) protocol. The ultrathin sections were expanded with chloroform vapor to minimize tissue compression. These sections were mounted on Formvar-coated grids (nos. 100 and 200 mesh) and stained for 2 min at room temperature in a lead citrate solution.

Analysis. The nerves were photographed using a Hitachi HU-11E electron microscope. Photomicrography sessions were not interrupted by grid holder or filament changes, and the microscope was left on continuously in order to minimize the possibility of a magnification change during sampling. Before and after each of the five micrography sessions, the image magnification was calibrated with carbon replica gratings (1134 and 2160 lines/mm) and carbon replica grids (4.665×10^6 grids/mm^2). This calibration procedure provides an estimate of the total sample area accurate to within 1.0%. The reference grid is specified as accurate to within 0.03% in a linear dimension (Ernest F. Fullam, Inc.).

The five estimates of optic nerve axon number are based on 783 sampling micrographs which were taken with strict reference to the grid bars. The fields we photographed were distributed uniformly across the entire section, although the grid bars prevented the sample from being truly uniform. Such a sampling protocol has been shown to maximize count accuracy (Elias and Hyde, 1980; D. M. Hyde, personal communication). With one exception, no sampling bias was introduced during photography, and thus no bias correction factors needed to be calculated. In one case, UNI-B, we avoided photographing a field if it included a blood vessel lumen with a diameter above 7.5 μm. As 2.0% of this section area

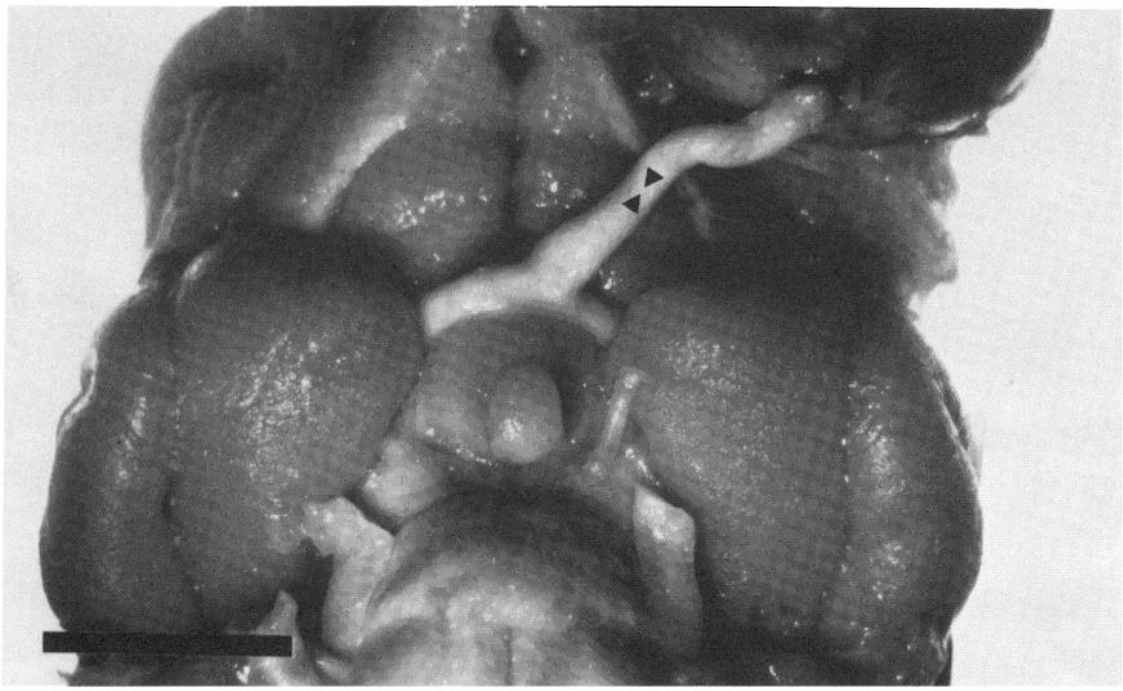

Figure 1. Ventral surface of the brain of a cat that had one eye removed more than 2 weeks before birth. The optic nerve emerges from the remaining eye as shown in the *upper right corner* of the photograph. A majority of fibers cross over the midline to form the contralateral optic tract. The *black triangles* point at the location at which the ultrathin sections of the nerve were taken. The *scale bar* represents 1 cm.

consisted of lumens with diameters above 7.5 μm, an area reduction factor of 0.98 was introduced. Other investigators (Stone and Campion, 1978) have biased their sampling against both blood vessels and large glial processes. This reduces the number of micrographs required to adequately sample the nerve face, but the necessary estimation of appropriate correction factors can be problematic.

The area of each ultrathin section was measured directly from a complete low power montage of the nerve as described by Easter et al. (1981). These montages were made using micrographs taken with a Zeiss EM 109 at the × 150 setting. The epineurium was not included in the area measurements. In addition, all section areas were estimated using an indirect method described by Vaney and Hughes (1976) which is based on the area of an adjacent 1-μm-thick section. This indirect method relies on an assessment of tissue compression which occurs while cutting the ultrathin sections. In our experience, tissue compression is not uniform, and as a result, the indirect method yields areal estimates in error by as much as 5%.

Photographic negatives (10.2 × 8.3 cm) were printed on sheets of Kodak RC II type F paper at an enlargement ratio of 2.4. Counts were made on these prints using the protocol of Gundersen (1977) which compensates for the micrograph edge effect. Each complete axon profile and all partial profiles which only abutted either the upper or right edge of the print were included in the count. All micrographs were checked at least twice to minimize count error. Estimates of the number of axons were determined by multiplying the total axon count of the micrograph series by the ratio of the thin section area to the sample area.

The adequacy of the sampling protocol was checked by dividing each pool of micrographs into four independent subsamples (subsample size ranged from 29 to 57 micrographs). Each of these subsamples was also distributed uniformly with one-fourth the spatial resolution of the full sample. Estimates based upon these partial samples typically were within 4% of the full sample values. However, the E-48 nerve showed an average estimate difference of 10% reflecting a high count variability. In general, our analysis showed that estimates based on a uniform sampling technique are relatively robust (cf. Snedecor and Cochran, 1972).

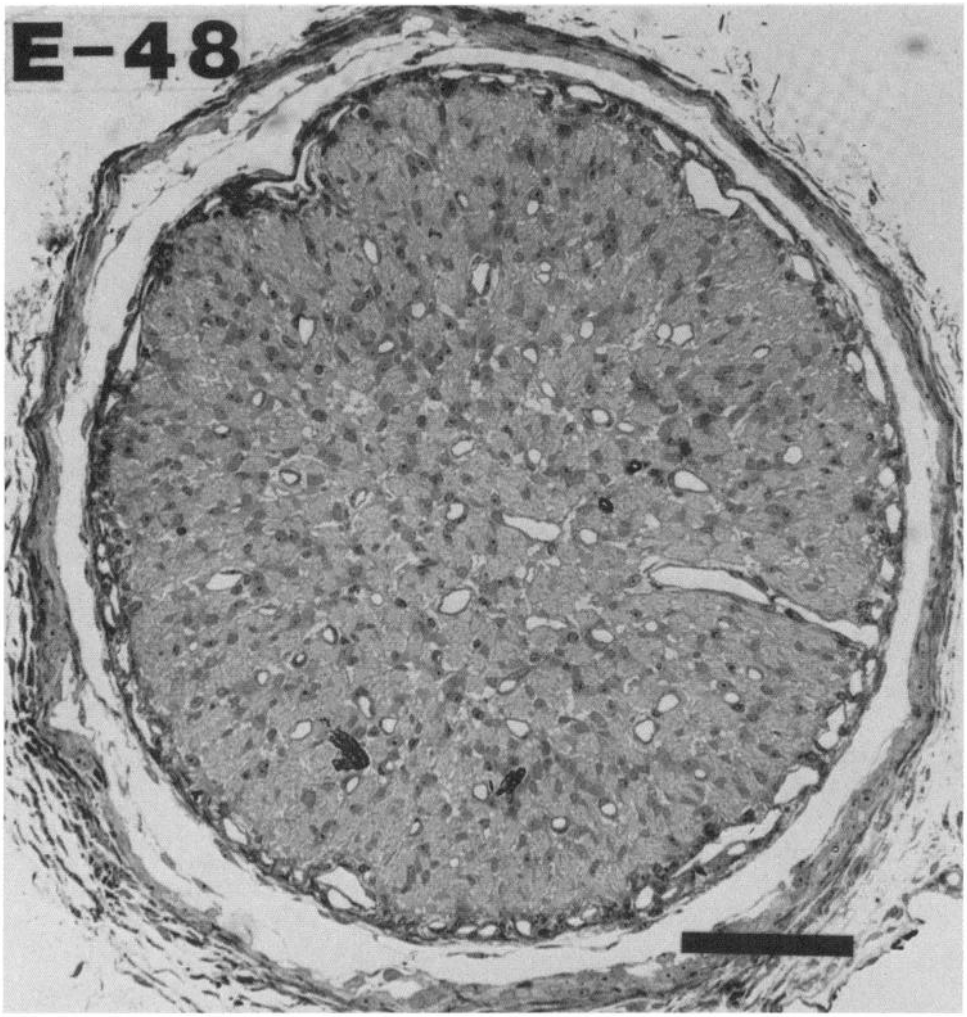

Figure 2. Fetal optic nerve section. In this 1-μm-thick section, immature glia are heavily stained. Lightly stained regions represent both the lumens of blood vessels and extracellular cisternae. Light gray regions consist of fascicles of unmyelinated axons (see Figs. 3 and 4). The *scale bar* equals 100 μm.

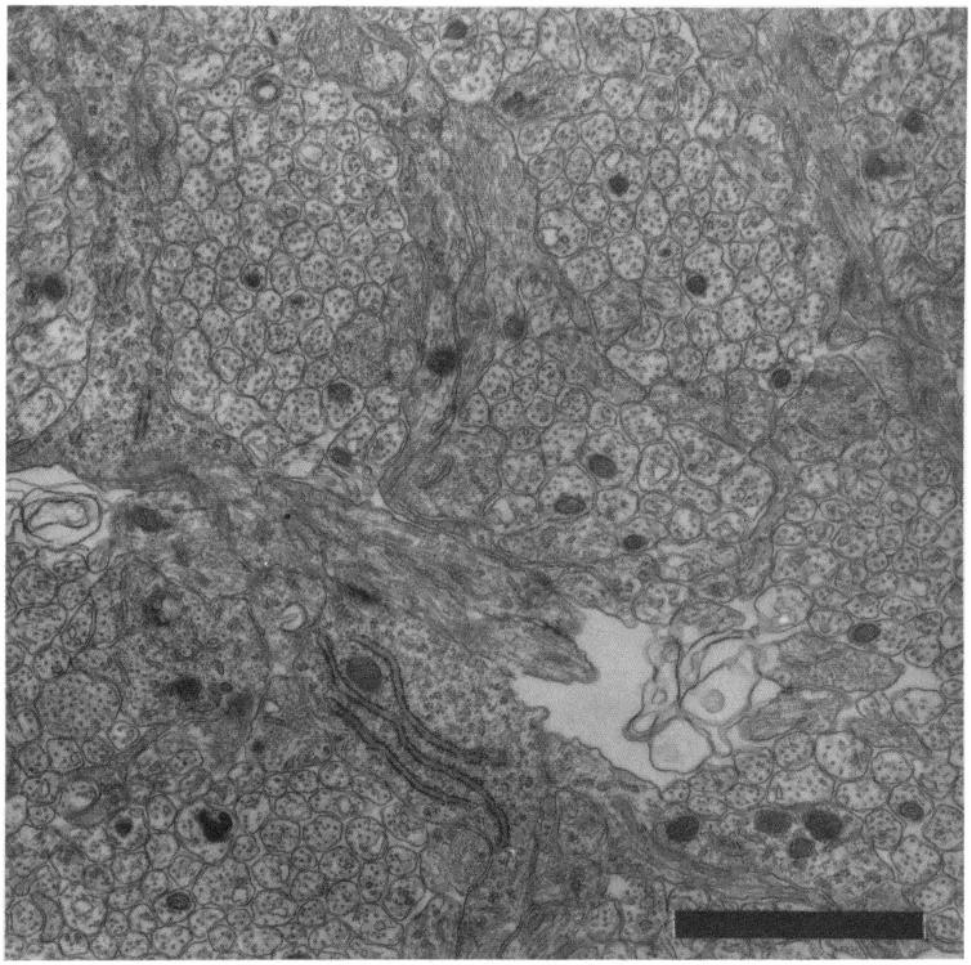

Figure 3. Fetal retinal ganglion cell axons in the optic nerve. Clusters of unmyelinated axons are separated by glial protrusions. Axons have a light cytoplasm containing an array of prominent microtubules, densely stained mitochondria, and smooth endoplasmic reticulum. The glial cytoplasm, on the other hand, is characterized by a rough endoplasmic reticulum, rosettes of ribosomes, and dense aggregates of fine filaments. Note the small extracellular space in the *lower right quandrant* of the micrograph. The *scale bar* represents 2 μm.

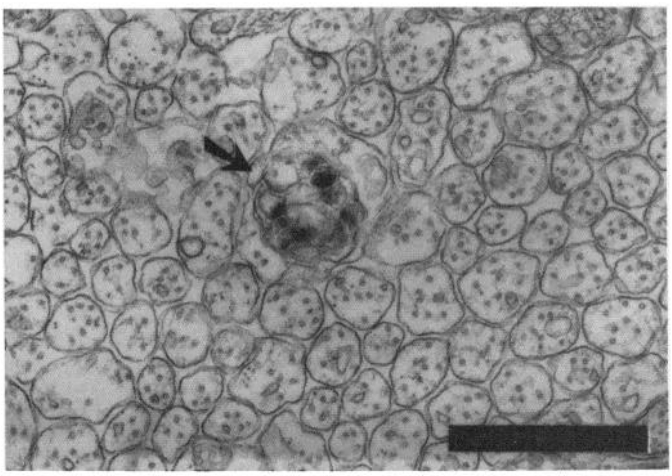

Figure 4. Dying retinal ganglion cell axon. The *arrow* points to the dense and mottled region which appears to be a necrotic axon. Surrounding axons appear normal. The *scale bar* equals 1 μm.

Results

A 1-μm-thick cross-section of the fetal optic nerve is shown in Figure 2. The dark glial cells are particularly prominent at this age. Compared to the adult, a large portion of the nerve is taken up by blood vessels and extracellular space. Electron micrographs of this nerve are shown in Figures 3 and 4. At E-48, numerous dark astrocytic protuberances penetrate through tightly packed fascicles of unmyelinated axons. No myelin is present. The axon diameter distribution was unimodal with a range from 0.1 to 0.6 μm and a mode at 0.3 μm (Chalupa et al., 1982). Of the 25,000 axons counted in this fetal nerve, only 2 appeared clearly necrotic (Fig. 4). Another 5 had particularly dense or mottled axoplasm, but whether these profiles were truly degenerative is not known. No growth cone profiles were noted in this survey. At E-48, glial cytoplasm appears particularly dense due to a high concentration of ribosome rosettes, abundant granular endoplasmic reticulum, and bundles of glial

filaments. Large extracellular cisternae were noted throughout the section as may be seen in Figures 2 and 3.

The appearance of the optic nerves of the experimental animals did not differ significantly from that of control nerves. Micrographs from UNI-A and UNI-B are shown in Figure 5, *A* and *B*. Unmyelinated profiles make up less than 1% of the count and probably represent axons sectioned at nodes. The range of axon sizes is similar to those reported by others (Friede et al., 1971; Hughes and Wässle, 1976; Moore et al., 1976; Freeman, 1978). The diameters, excluding the sheath, averaged 1.6 μm with minima and maxima of 0.3 and 8.0 μm.

Photographs of a 1-μm-thick section and the adjacent ultrathin section on a no. 200 mesh grid from animal UNI-A are shown in Figure 6, *A* and *B*. Individual large axons can be identified in both of these photographs. In fact, the large axons in Figure 5*A* can be recognized in the grid window of Figure 6*B* marked with a *star*. The difference in the shape of these two cross-sections is due to tissue deformation during ultramicrotomy (see "Materials and Methods"). In the montage of the ultrathin section (Fig. 6*B*), the grid window size is 8100 μm^2 (90 × 90 μm) and the bar width is 37 μm. A single micrograph covering 1274 μm^2 was taken from each of the 119 grid windows. The spatial distribution of axon counts in these micrographs provides an index of fiber packing density as a function of eccentricity. Figure 6, *C* and *D*, shows the distribution of counts across the section of UNI-A. In figure 6*C*, the lowest axon count in one micrograph is 69, the highest is 232. The mean count is 133 with a standard deviation of 36. In Figure 6*D* the counts have been divided into six classes, each with a range of 1 SD. Class 6, for example, contains the two highest counts (213 and 232) and is represented by the largest sized *circle*. Figures 7 and 8 provide a similar graphic summary of the count distribution for the four other nerve sections. From this figure it is apparent that the highest axon packing density generally is found within a peripheral crescent of the nerve. This is particularly evident in the sections from UNI-B (Fig. 7*A*) and from the adult control nerves (Fig. 8). High peripheral counts are also evident in the E-48 section (Fig. 7*B*). The UNI-A section (Fig. 6*D*) appears exceptional because of its comparatively high central counts. However, this section was taken within 0.5 mm of the head of the optic nerve, while all other sections originate from intermediate portions of the nerve. Collectively, the density maps indicate that axon packing is not uniform in the optic nerve. High axonal densities may be due to the inclusion of many small diameter axons, and conversely, areas of lower axon counts may result from the predominance of large caliber fibers. It is also possible that the axon packing density gradients simply reflect local differences in glial volume and are not related to regional variation in mean axon diameter. A regional analysis of fiber caliber would resolve this issue (R. W. Williams and L. M. Chalupa, submitted for publication).

Table I provides the pertinent numerical data on the five optic nerve sections and the resulting estimates of axon number. The E-48 fetal nerve was estimated to have 328,000 ± 17,500 axons. The two normal adult nerves contained 159,000 ± 3,400 and 158,000 ± 4,000 fibers, whereas the remaining nerves of the two unilaterally enucleated cats contained 198,000 ± 4,800 and 200,000 ± 4,700 fibers. If it is assumed that the control and experimental populations are distributed normally with similar variability, then the differences in axon population estimates between the groups are statistically significant ($t = 36.2$, $p < 0.005$, $df = 2$, two-tailed test).

Discussion

The results of this study establish that there are substantially more ganglion cell axons in the fetal than in the adult cat optic nerve and, furthermore, that the normal loss of ganglion cell axons is caused, at least in part, by prenatal binocular competition since *in utero* removal of one eye increases the number of axons in the remaining nerve. Although these findings admittedly are based on a limited sample, the low variability in both experimental and control groups resulted in a statistically significant difference, and thus we are reasonably confident that our main conclusions are justified.

Our estimates of axon number in the normal adult cat are higher than previous estimates based on light microscopic counts (Bruesch and Arey, 1942; Donovan, 1967), presumably due to the inclusion in our counts of the smallest axons. Two recent papers have estimated axon number within the optic nerve of the adult cat using electron microscopic techniques. Hughes and Wässle (1976) examined two optic nerves in detail and estimated that they were comprised of 179,000 and 188,000 axons (estimates weighted for eccentricity). Stone and Campion (1978), on the other hand, examined four nerves and concluded the mean number of ganglion cell axons to be approximately 130,000 with a range from 112,800 to 147,200. We were concerned by this discrepancy, particularly since this order of variability could easily obscure any effect of prenatal unilateral enucleation on the axon population. The basis for the discrepancy is not clear (but see the discussion of Stone and Campion, 1978). We believe that the sampling protocols employed by Hughes and Wässle (1976) and by Stone and Campion (1978) could have yielded unreliable estimates of the number of axons within the optic nerve, because in both of these studies electron micrographs typically were taken along two or more diameters of the nerve section. As a result, more micrographs were obtained from central than from peripheral sites. For example, eight micrographs were taken within the central core of the nerve illustrated in Figure 2, section C of Hughes and Wässle (1976), although this core region makes up only 4.5% of the total area. Seven micrographs, however, were taken within the peripheral rind which comprises 35% of the area. Our results, as well as those of Vaney and Hughes (1976), clearly demonstrate that axonal packing density is neither a function of axis nor eccentricity. For this reason it is difficult to correct estimates based on a centrally biased sample simply by giving more weight in the final calculation to the peripheral counts. Using the sampling protocol typically employed by Hughes and Wässle (1976)

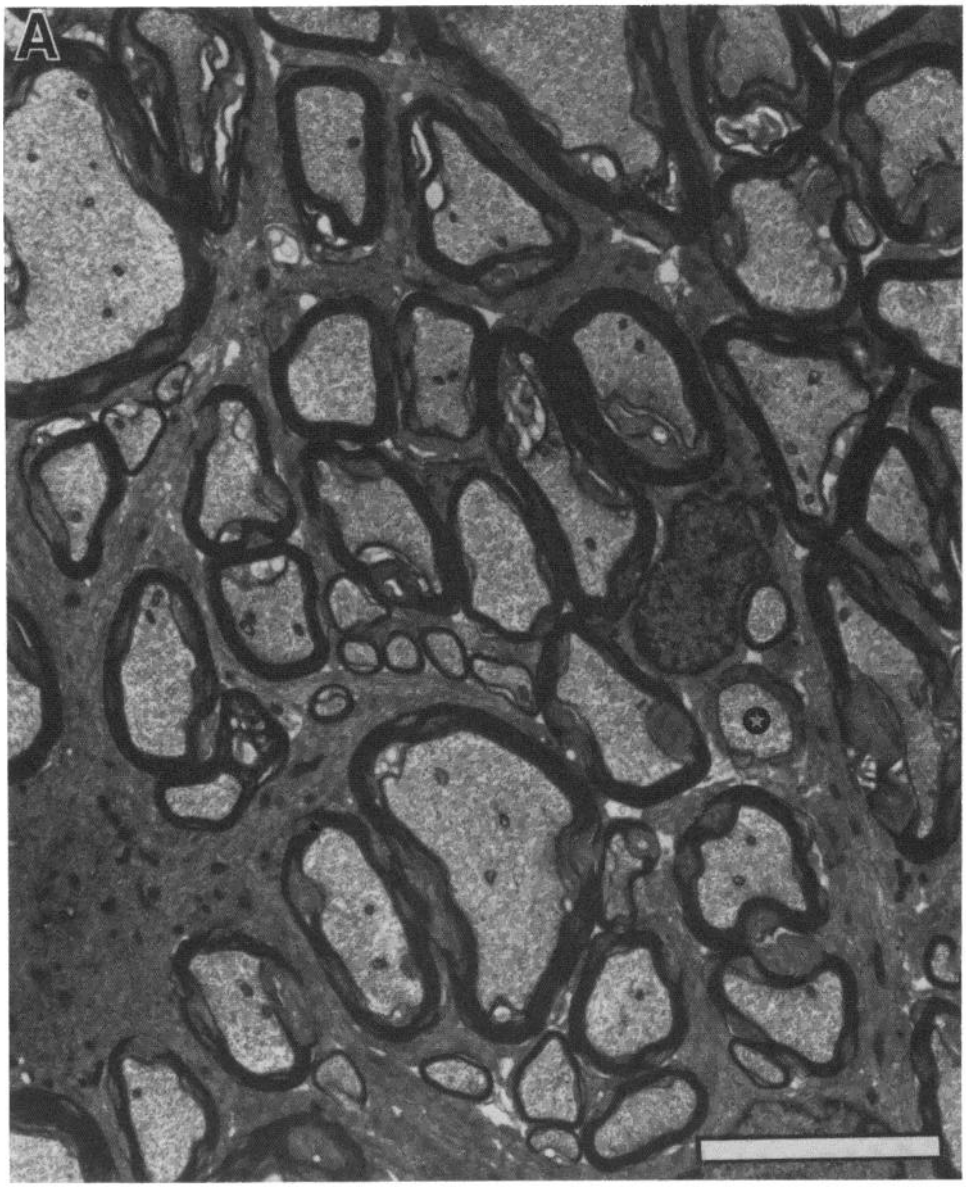

Figure 5. Retinal ganglion cell fibers in the unilateral enucleate cats, UNI-A (*A*) and UNI-B (*B*). All axons are myelinated. Fibers cut close to nodes of Ranvier are marked with *stars*. The myelin sheaths are partially delaminated, due in large part to our fixation procedures. The *calibration bar* in *A* is 5 μm and in *B* is 2 μm.

and Stone and Campion (1978), we found that two pairs of orthogonal diameter samples gave estimates which varied by as much as 20%. This may, in part, explain the disagreement between the previous estimates. It is of interest to note that a recent study by Illing and Wässle (1981) concluded that there are about 151,000 ganglion cells in the normal adult cat retina. This estimate closely matches that which we have obtained for the number of axons within the optic nerves of our control animals.

The normal developmental loss of optic nerve axons and the moderation of this loss following the early elimination of binocular competition are explicable by at least two mechanisms: retinal ganglion cell death and the regression of axon collaterals within the optic nerve. If a substantial number of retinal ganglion cell axons branched in the retina or nerve of the fetal cat, then prenatal unilateral enucleation could stabilize these collaterals without necessarily affecting the ganglion cell population. To our knowledge, axon bifurcation within the retina or optic nerve has not been reported in any species of adult vertebrate. Furthermore, in studies of the developing vertebrate retina (for example, Morest, 1970; Goldberg and Coulombre, 1972; Ramón y Cajal, 1972; Hinds and Hinds, 1974; Nishimura, 1980) there have been no reports of ganglion cells with multiple or bifurcating axons. Thus, it is difficult to evaluate the merits of this hypothesis until more information is available on the detailed morphology of individual developing feline ganglion cells. An alternative strategy to answer this question would involve a retinal whole mount study

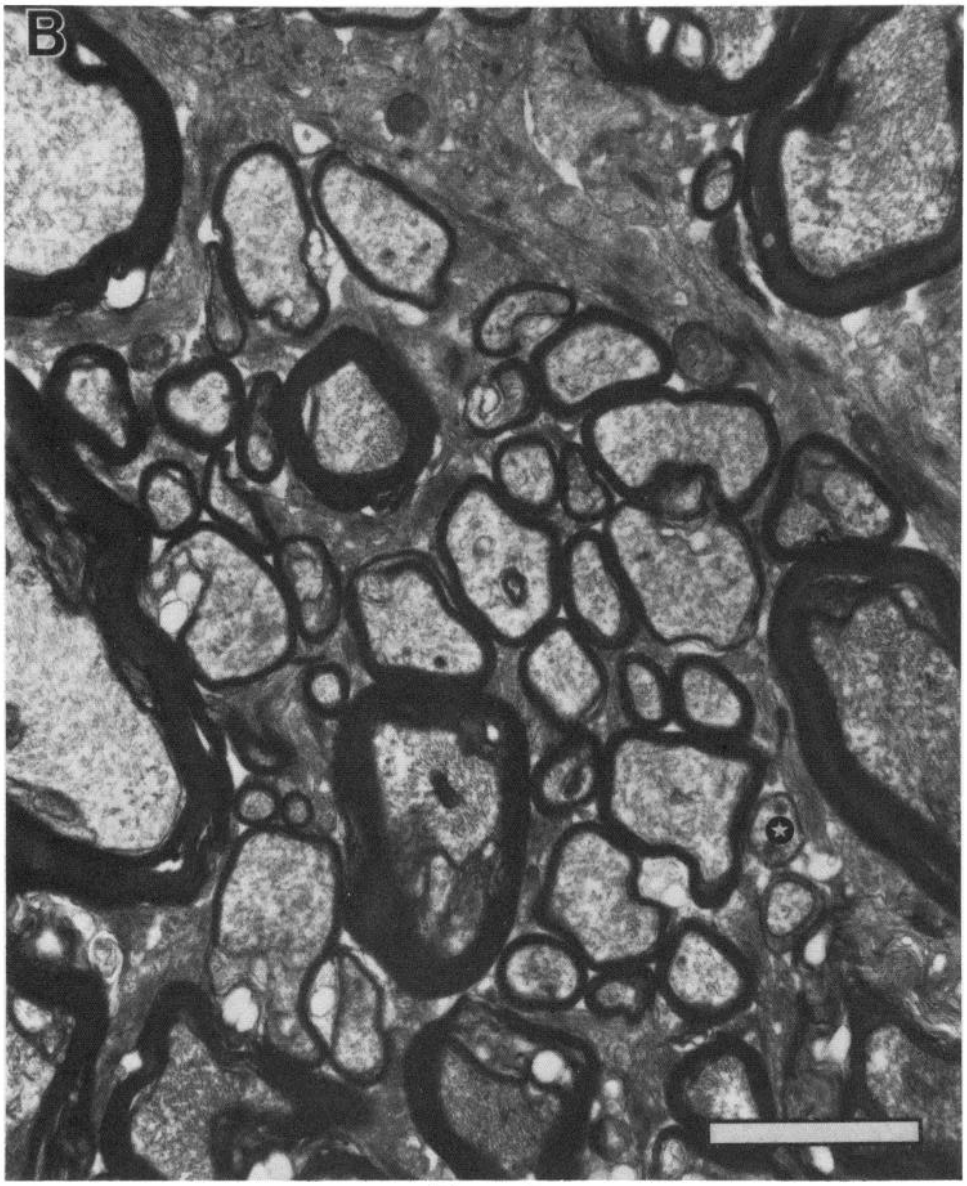

Figure 5B.

of mature animals that had one eye removed *in utero*. If the estimate of the ganglion cell soma population matched that of the optic nerve axon population provided by the present study, then the branched axon hypothesis could be rejected unequivocally.

Several recent studies have shown that neuronal loss occurs in the mammalian retina (Kuwabara and Weidman, 1974; Jeffery and Perry, 1981; Sengelaub and Finlay, 1981, 1982; Cunningham et al., 1981). Most pertinent to the present study is the work of Stone et al. (1982) who examined Nissl-stained retinal whole mounts of fetal, neonatal, and adult cats and estimated that there were about 6 times as many young neurons in the ganglion cell layer of an E-47 fetus as in the adult. However, as noted by these investigators, it is very difficult to differentiate small immature neurons in the incipient ganglion cell layer from glial cells. Furthermore, amacrine cells may be derived from precursors which resemble early ganglion cells (Hinds and Hinds, 1974, 1978). Both of these factors could lead to spuriously high estimates of ganglion cell number in the fetal retina. Indeed, our results indicate that this is the case, since we obtained only a 2-fold difference in the number of ganglion cell axons between E-48 and maturity. It is now of obvious interest to determine the time course of ganglion cell axon loss in the cat, as has been done in the chick (Rager and Rager, 1976) and the primate (Rakic and Riley, 1982).

Reduction of neuron death generally is contingent on an increase in available target sites (Hamburger, 1939; Hollyday and Hamburger, 1976; Boydston and Sohal, 1979; Lamb, 1979; Oppenheim, 1981). Particularly relevant to the present study are the findings of Rakic (1979, 1981) who showed that fetal unilateral enucleation in the monkey doubles the terminal volume available to the spared eye. Furthermore, the synaptic structure within the dorsal lateral geniculate of these monocular monkeys

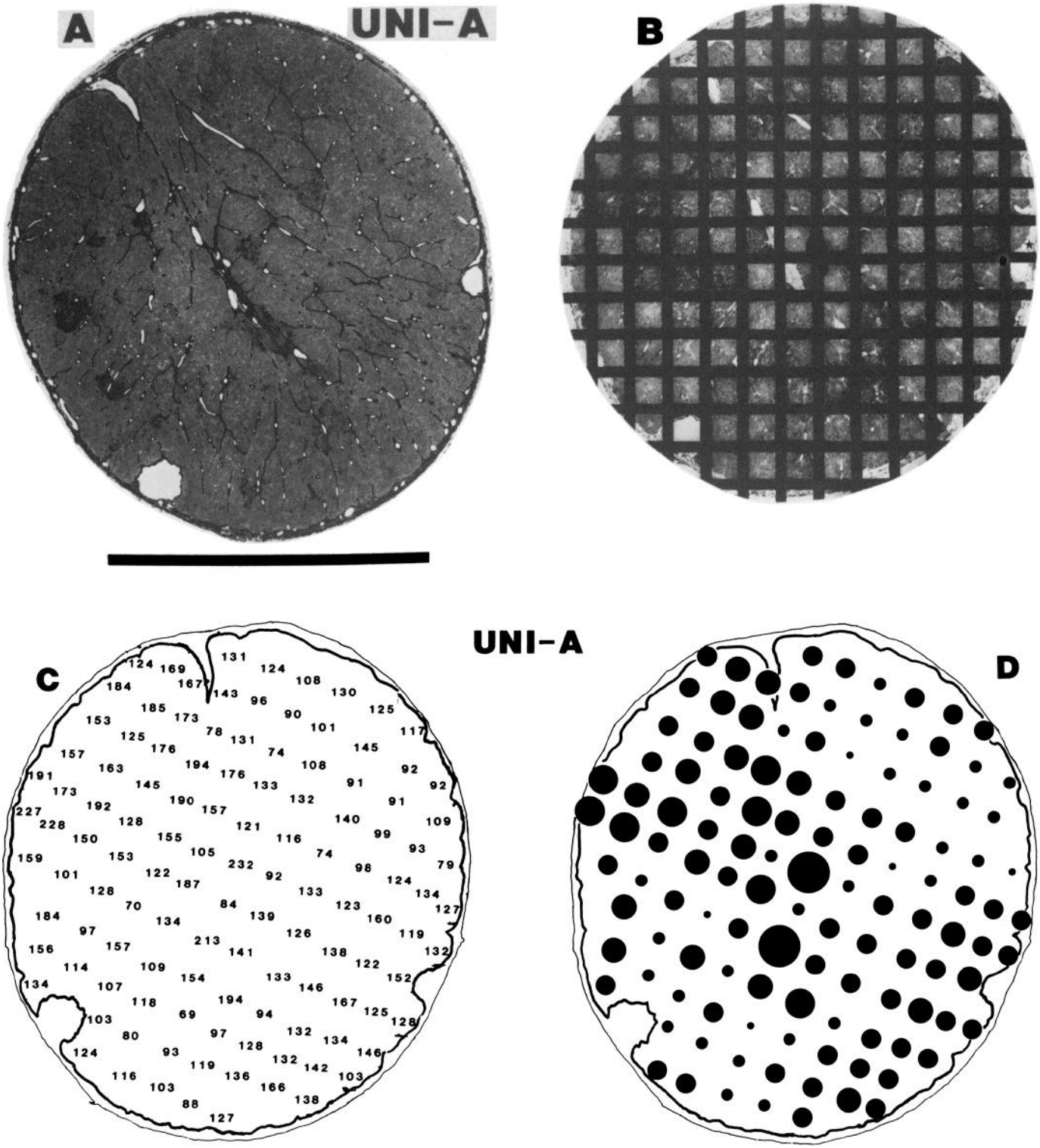

Figure 6. The optic nerve of the experimental animal UNI-A. This cat had one eye removed on gestational day E-45 and was sacrificed more than 7 months later. *A*, A 1-μm-thick section of the nerve. The epineurial sheath and other fibrous regions are heavily stained. Large axons are clearly distinguishable. Note the oval shape of this section and compare to that of the ultrathin section depicted in *B*. The *scale bar* represents 1 mm. *B*, A low power electron micrograph montage of the UNI-A section. This montage, made up from 20 individual negatives, was used to determine the section area. The epineurial sheath as well as the three large peripheral blood vessels were not included in the measurement of area. Individual axons, identified in *A*, can be easily located in *B*. A segment of the nerve in the grid window marked with a *star* can be recognized in Figure 5*A*. The *scale* is the same as in *A*: grid windows are 90 × 90 μm. *C*, The number of axons counted in each of 119 micrographs taken of the section shown in *B* are superimposed on a sketch of the nerve. A total of 15,786 fibers were counted. *D*, Map of axon packing density. The numbers shown in *C* were divided into six classes, each represented by a different size of *black circle* (see "Results" for further details). Regions of high axon density are represented by *large circles*.

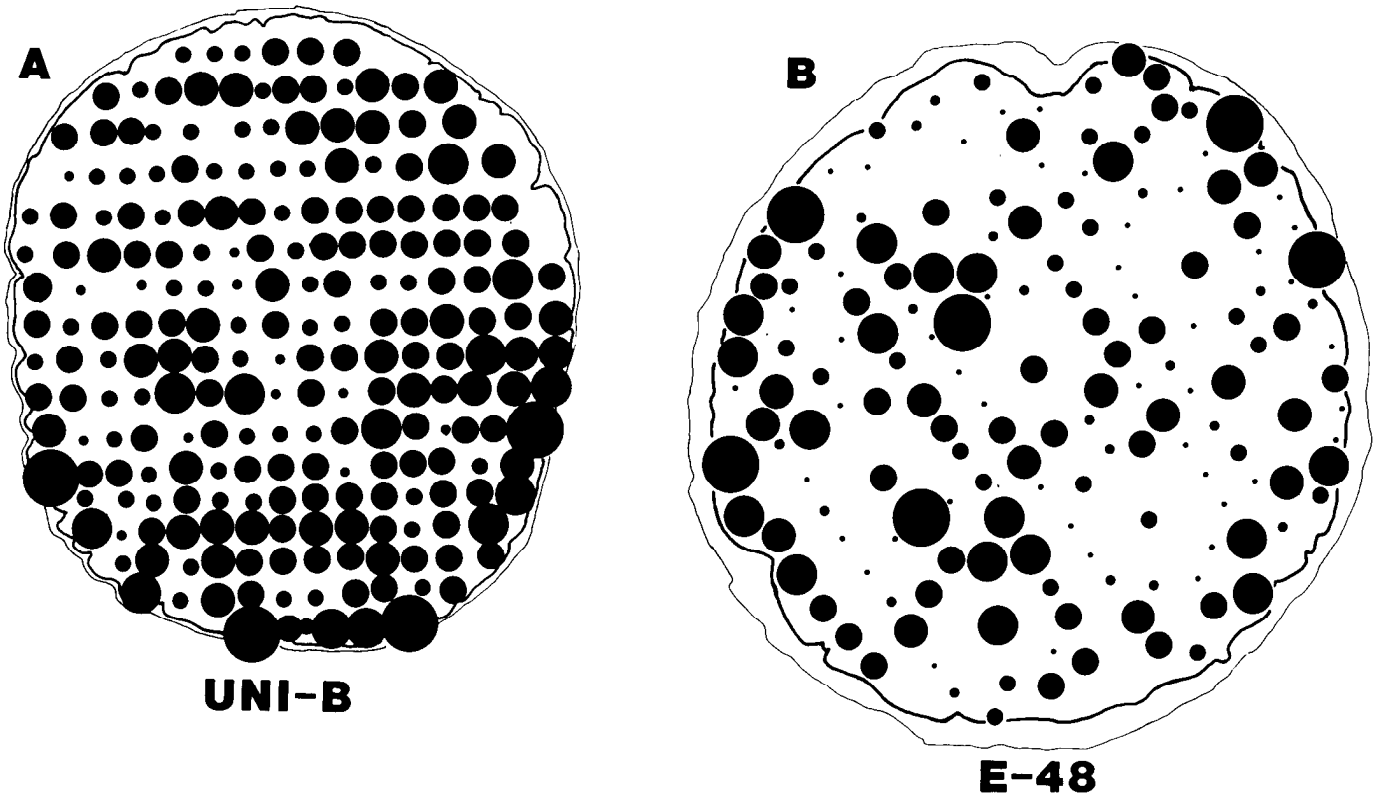

Figure 7. Maps of axon packing density for the experimental cat UNI-B (*A*) and for the E-48 fetus (*B*). In *A*, the conventions are identical to those of Figure 6*D*. A total of 8,555 axons were counted in 228 micrographs. In Figure 8*B*, seven circle sizes were used. Each class includes counts with a range of one-half of a standard deviation. The standard deviation of axon counts in this fetus was 103 axons. A total of 25,033 axons were counted in 168 micrographs.

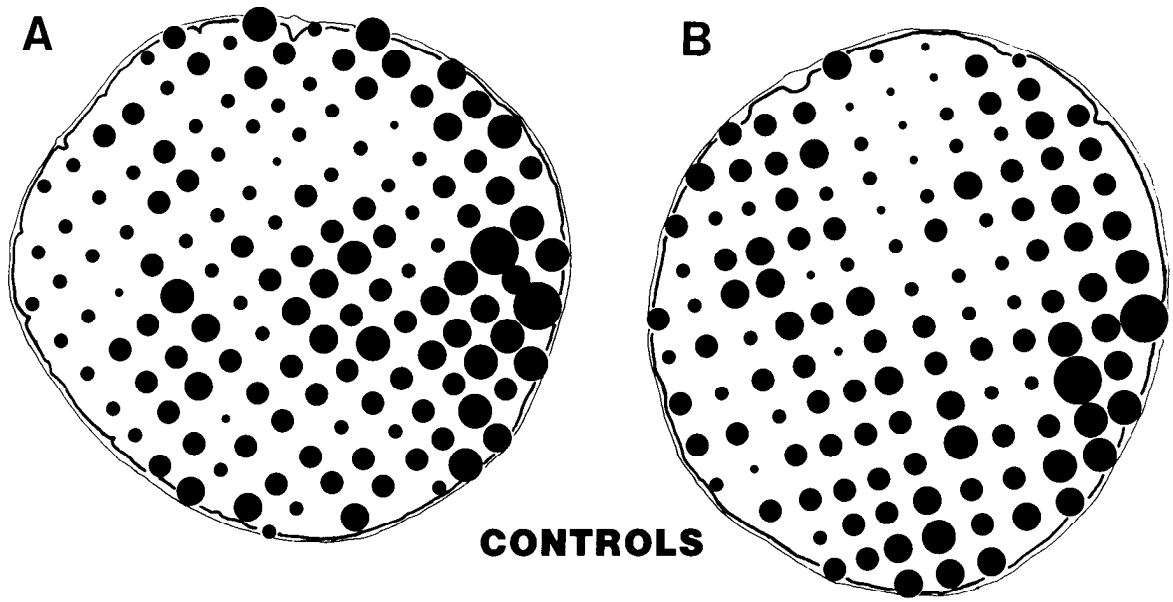

Figure 8. Maps of axon packing density for the two control cat optic nerve sections. Conventions are as in Figure 6*D*. Each map was rotated to bring the region of highest packing density to the 3 o'clock position. In these two maps a peripheral crescent of the nerve section appears to contain a disproportionate number of fibers. In *A*, 13,318 fibers were counted in 139 micrographs. In *B*, 13,751 fibers were counted in 129 micrographs.

appeared to be normal. Given Rakic's findings, we anticipated that fetal unilateral enucleation would largely prevent neuron or axon loss of the remaining eye. However, we found that the normal 50% attrition of the primordial axon population was only attenuated by about 12%, resulting in a population 25% above normal. It is, of course, possible that unilateral eye extirpation in the prenatal cat exacerbates the incidence of neuron loss in

TABLE I

Estimates of fiber number within the optic nerve

The table gives a summary of measurements and counts used to estimate the total axon population of the optic nerves of two normal cats, two experimental cats, UNI-A and UNI-B, which each had one eye removed more than 2 weeks before birth, and a 48-day fetus.

Cat Number and Age at Sacrifice	Total Axon Number[a]	Number of Axons Counted	Area of Ultrathin Section	Average Area Covered by Micrograph	Number of Micrographs	Nerve Area Sampled
			mm^2	μm^2		%
Control no. 1, 10 months	159,000 ±3,400	13,751	1.95	1304	129	8.6
Control no. 2, 18 months	158,000 ±4,000	13,318	2.11	1282	139	8.4
UNI-A, 218 days	198,000 ±4,800	15,786	1.90	1274	119	8.0
UNI-B, 75 days	200,000 ±4,700	8,555	1.43	263.6	228	4.3
Fetus, E-48	328,000 ±17,500	25,033	0.149	67.37	168	7.6

[a] Estimates are rounded to the nearest thousand. The confidence intervals are based on the standard error of the mean of the set of micrograph axon counts taken from each animal. Thus, the interval is an indicator of the degree of sampling error and does not include possible errors attributable to either miscounting of axons or to inaccuracy in the measurements of nerve and micrographs areas (refer to "Materials and Methods" for details of counting and measurement procedures).

the terminal nuclei (cf. Cowan, 1973). If this loss were accompanied by either increase in glial proliferation or glial hypertrophy, then the overall terminal volume would not be reduced appreciably, while the number of available postsynaptic sites would decrease. In addition, it is possible that the residual ganglion cell axon loss which is not affected by reduced binocular competition may be dependent on intraretinal events, such as synaptogenesis in the inner plexiform layer.

The role of axon loss in the normal development of the retinofugal projection is unknown. At least three contributions can be envisioned. First, this attrition may underlie the development of discrete ocular dominance domains in the lateral geniculate and superior colliculus. This view is supported by our finding that the magnitude of axon loss is reduced by unilateral enucleation. Second, the loss may be related to a refinement of visual field topography within the terminal nuclei. The topographic organization of the prenatal cat's visual system is yet to be studied. However, in a previous investigation, we (Williams and Chalupa, 1982a) demonstrated that at E-38 and E-46 the ipsilateral retinotectal projection in the cat extends to the caudal portion of the superior colliculus. Since this region represents the monocular crescent of the contralateral visual hemi-field in the adult, it is apparent that the early retinotectal projection does not have the same topographic organization as that of the mature animal. Thus, the elimination of ganglion cell axons which arborize within topographically incongruent fields could contribute to the acquisition of retinotopic order (cf. Clarke and Cowan, 1976; McLoon, 1982). Similarly, axon loss could reflect the elimination of projections to inappropriate target structures, such as the limited, transient retino-retinal pathway which has recently been described in rat embryos (Bunt and Lund, 1981). Third, ganglion cell axon loss may contribute to the functional segregation of retinofugal projections. The feline retinal ganglion cell population has been grouped into three classes (X, Y, and W) using physiological and morphological criteria (for reviews see Rodieck, 1979; Stone et al., 1979). In the adult cat, each of the retinorecipient nuclei receives a unique distribution of input from the three classes. Whether this is also the case in the prenatal animal is unknown, but clearly, axon retraction or ganglion cell death could serve to eliminate an abnormal class of early input to a given target structure. This problem can be addressed by studying the response properties of neurons within the lateral geniculate and the superior colliculus in mature cats that had one eye removed *in utero*. Ongoing studies in this laboratory (Williams and Chalupa, 1982b) have shown that in such animals the remaining retina is capable of driving visual cells in all regions of the contralateral and ipsilateral lateral geniculate nucleus. It is yet to be determined, however, whether the functional segregation of cell type, so prominent in the normal adult, is also present in the prenatally enucleated animals.

References

Boydston, W. R., and G. S. Sohal (1979) Grafting of additional periphery reduces embryonic loss of neurons. Brain Res. *178:* 403–410.

Bruesch, S. R., and L. B. Arey (1942) The number of myelinated and unmyelinated fibers in the optic nerve of vertebrates. J. Comp. Neurol. *77:* 631–656.

Bunt, S. M., and R. D. Lund (1981) Development of a transient retino-retinal pathway in hooded and albino rats. Brain Res. *211:* 399–404.

Cavalcante, L. A., and C. E. Rocha-Miranda (1978) Postnatal development of retinogeniculate, retinopretectal and retinotectal projections in the opossum. Brain Res. *146:* 231–248.

Chalupa, L. M., R. W. Williams, and M. J. Bastiani (1982) Bimodality of axon size in the cat optic nerve: A quantitative electron microscopic analysis. Soc. Neurosci. Abstr. *8:* 203.

Clarke, P. G. H., and W. M. Cowan (1976) The development of the isthmo-optic tract in the chick, with special reference to the occurrence and correction of developmental errors in the location and connection of isthmo-optic neurons. J. Comp. Neurol. *167:* 143–164.

Cowan, W. M. (1973) Neuronal death as a regulative mechanism in the control of cell number in the nervous system. In

Development and Aging in the Nervous System, M. Rockstein, ed., pp. 19–41, Academic Press, New York.

Cunningham, T. J., C. Huddelston, and M. Murray (1979) Modification of neuron numbers in the visual system of the rat. J. Comp. Neurol. *184:* 423–434.

Cunningham, T. J., I. M. Mohler, and D. L. Giordano (1981) Naturally occurring neuron death in the ganglion cell layer of the neonatal rat: Morphology and evidence for regional correspondence with neuron death in superior colliculus. Dev. Brain Res. *2:* 203–215.

Donovan, A. (1967) The nerve fibre composition of the cat optic nerve. J. Anat. *101:* 1–11.

Easter, S. S., Jr., A. C. Rusoff, and P. E. Kish (1981) The growth and organization of the optic nerve and tract in juvenile and adult goldfish. J. Neurosci. *1:* 793–811.

Elias, H., and D. M. Hyde (1980) An elementary introduction to stereology (Quantitative microscopy). Am. J. Anat. *159:* 411–446.

Freeman, B. (1978) Myelin sheath thickness and conduction latency groups in the cat optic nerve. J. Comp. Neurol. *181:* 183–196.

Friede, R. L., T. Miyaghishi, and K. H. Hu (1971) Axon calibre, neurofilaments, microtubules, sheath thickness and cholesterol in cat optic nerve fibres. J. Anat. *108:* 365–373.

Frost, D. O., K. -F. So, and G. E. Schneider (1979) Postnatal development of retinal projections in the Syrian hamster: A study using autoradiographic and anterograde degeneration techniques. Neuroscience *4:* 1649–1677.

Goldberg, S., and A. J. Coulombre (1972) Topographical development of the ganglion cell fiber layer in the chick retina. A whole mount study. J. Comp. Neurol. *146:* 507–518.

Gundersen, H. J. G. (1977) Notes on the estimation of the numerical density of arbitrary profiles: The edge effect. J. Microsc. *111:* 219–223.

Hamburger, V. (1939) Motor and sensory hyperplasia following limbbud transplantation in chick embryos. Physiol. Zool. *12:* 268–284.

Hinds, J. W., and P. L. Hinds (1974) Early ganglion cell differentiation in the mouse retina: An electron microscopic analysis utilizing serial sections. Dev. Biol. *37:* 381–416.

Hinds, J. W., and P. L. Hinds (1978) Early development of amacrine cells in the mouse retina: An electron microscopic, serial section analysis. J. Comp. Neurol. *179:* 277–300.

Hollyday, M., and V. Hamburger (1976) Reduction of the naturally occurring motor neuron loss by enlargement of the periphery. J. Comp. Neurol. *170:* 311–320.

Hughes, A., and H. Wässle (1976) The cat optic nerve: Fibre total count and diameter spectrum. J. Comp. Neurol. *169:* 171–184.

Illing, R. -B., and H. Wässle (1981) The retinal projection to the thalamus in the cat: A quantitative investigation and a comparison with the retinotectal pathway. J. Comp. Neurol. *202:* 265–285.

Jeffery, G., and V. H. Perry (1981) Evidence for ganglion cell death during development of the ipsilateral retinal projection in the rat. Dev. Brain Res. *2:* 176–180.

Kliot, M., and C. J. Shatz (1981) Siamese cat: Prenatal development of the retinogeniculate pathway. Invest. Ophthalmol. Vis. Sci. (Suppl.) *20:* 175.

Kuwabara, T., and T. A. Weidman (1974) Development of the prenatal rat retina. Invest. Ophthalmol. *13:* 725–739.

Lamb, A. H. (1979) Ventral horn cell counts in a *Xenopus* with naturally occurring supernumerary hindlimbs. J. Embryol. Exp. Morphol. *49:* 13–16.

Land, P. W., and R. D. Lund (1979) Development of the rat's uncrossed retinotectal pathway and its relation to plasticity studies. Science *205:* 698–700.

Linden, D. C., R. W. Guillery, and J. Cucchiaro (1981) The dorsal lateral geniculate nucleus of the normal ferret and its postnatal development. J. Comp. Neurol. *20:* 189–211.

McLoon, S. C. (1982) Alterations in precision of the crossed retinotectal projection during chick development. Science *215:* 1418–1420.

Moore, C. L., R. Kalil, and W. Richards (1976) Development of myelination in optic tract of the cat. J. Comp. Neurol. *165:* 125–136.

Morest, D. K. (1970) The pattern of neurogenesis in the retina of the rat. Z. Anat. Entwicklungsgesch. *131:* 45–67.

Nishimura, Y. (1980) Determination of the developmental pattern of retinal ganglion cells in chick embryos by Golgi impregnation and other methods. Anat. Embryol. (Berl.) *158:* 329–347.

Oppenheim, R. W. (1981) Neuronal cell death and some related regressive phenomena during neurogenesis: A selective historical review and progress report. In *Studies in Developmental Neurobiology: Essays in Honor of Viktor Hamburger*, W. M. Cowan, ed., pp. 74–133, Oxford University Press, Inc., New York.

Rager, G., and U. Rager (1976) Generation and degeneration of retinal ganglion cells in the chicken. Exp. Brain Res. *25:* 551–553.

Rakic, P. (1976) Prenatal genesis of connections subserving ocular dominance in the rhesus monkey. Nature *261:* 467–471.

Rakic, P. (1977) Prenatal development of the visual system in rhesus monkey. Philos. Trans. R. Soc. Lond. (Biol.) *278:* 245–260.

Rakic, P. (1979) Genesis of visual connections in the rhesus monkey. In *Developmental Neurobiology of Vision*, R. D. Freeman, ed., pp. 249–260, Plenum Press, New York.

Rakic, P. (1981) Development of visual centers in the primate brain depends on binocular competition before birth. Science *214:* 928–931.

Rakic, P., and K. P. Riley (1982) Number of axons in the optic nerve of the developing rhesus monkey: Overproduction and elimination before birth. Soc. Neurosci. Abstr. *8:* 814.

Ramón y Cajal, S. (1972) *The Structure of the Retina*, compiled and translated by S. A. Thorpe and M. Glickstein, Charles C Thomas, Springfield, IL.

Richardson, K. G., L. Jarrett, and E. H. Finke (1960) Embedding in epoxy resins for ultra thin sectioning in electron microscopy. Stain Technol. *35:* 313–323.

Rodieck, R. W. (1979) Visual pathways. Annu. Rev. Neurosci. *2:* 193–225.

Sengelaub, D. R., and B. L. Finlay (1981) Early removal of one eye reduces normally occurring cell death in the remaining eye. Science *213:* 573–574.

Sengelaub, D. R., and B. L. Finlay (1982) Cell death in the mammalian visual system during normal development. I. Retinal ganglion cells. J. Comp. Neurol. *204:* 311–317.

Shatz, C. J., and A. C. DiBerardino (1980) Prenatal development of the retinogeniculate pathway in the cat. Soc. Neurosci. Abstr. *6:* 485.

Snedecor, G. W., and W. G. Cochran (1972) *Statistical Methods*, pp. 504–539, Iowa State University Press, Ames.

Stone, J., and J. E. Campion (1978) Estimate of the number of myelinated axons in the cat's optic nerve. J. Comp. Neurol. *180:* 799–806.

Stone, J., B. Dreher, and A. Leventhal (1979) Hierarchical and parallel mechanisms in the organization of visual cortex. Brain Res. Rev. *1:* 345–394.

Stone, J., D. H. Rapaport, R. W. Williams, and L. M. Chalupa (1982) Uniformity of cell distribution in the ganglion cell layer of prenatal cat retina: Implications for mechanisms of

retinal development. Dev. Brain Res. *2:* 231–242.
Treff, W. M., E. Meyer-König, and W. Schlote (1972) Morphometric analysis of a fibre system in the central nervous system. J. Microsc. *95:* 337–343.
Vaney, D. I., and A. Hughes (1976) The rabbit optic nerve: Fibre diameter spectrum, fibre count, and comparison with a retinal ganglion cell count. J. Comp. Neurol. *170:* 241–252.
Williams, R. W., and L. M. Chalupa (1980) Projections of retinal ganglion cells in the fetal cat. Soc. Neurosci. Abstr. *6:* 492.
Williams, R. W., and L. M. Chalupa (1981) Prenatal development of retinal projections to the midbrain of the cat. Invest. Ophthalmol. Vis. Sci. (Suppl.) *20:* 74.
Williams, R. W., and L. M. Chalupa (1982a) Prenatal development of retinocollicular projections in the cat: An anterograde tracer transport study. J. Neurosci. *2:* 604–622.
Williams, R. W., and L. M. Chalupa (1982b) The effects of prenatal unilateral enucleation upon the functional organization of the cat's lateral geniculate nucleus. The Physiologist *25:* 223.